17th World Conference on Earthquake Engineering, 17WCEE
Sendai, Japan - September 13th to 18th 2020

GROUND MOTION INTENSITY PREDICTION STUDY OF HIGH PROBABILITY DESTRUCTIVE ESRTHQUAKES IN XICHANG AREA

Zongchao.Li(1), Xueliang.Chen(2), Jize.Sun(3), Hong.Zhou(4), Guochen.Wang(5), Qing.Wu(6)

(1) Ph.D, Institute of Geophysics, China Earthquake Administration, lizongchaoigo@163.com
(2) Ph.D, Institute of Geophysics, China Earthquake Administration, chenxueliang007@126.com@126.com
(3) Ph.D, Institute of Geophysics, China Earthquake Administration, sun_jize@126.com
(4) Ph.D, Institute of Geophysics, China Earthquake Administration, zhouhong@cea-igp.ac.cn
(5) Lecturer, Ludong University, 303304666@qq.com
(6) Ph.D, Institute of Geophysics, China Earthquake Administration, wuqing908@sina.com

Abstract

An earthquake of Magnitude 5.1 occurred in Xichang County, Liangshan Yi Autonomous Prefecture, Sichuan Province (27.70 N, 102.08 E) on Oct. 31st, 2018. This paper, with an analysis of this minor earthquake, intends to reveal the ground motion intensity characteristics of magnitude 7.5 earthquake in Xichang County since 1850. There is a strong correlation between the ground motion intensity characteristics and the distribution of asperity. Asperity is the main area of energy release. The accuracy of the selection of asperity parameters has a great influence on the prediction results of ground motion. At present, in the numerical simulation of ground motion, the establishment of source model and the study of the application of the ground motion prediction results in practical engineering, the accuracy of relevant parameters of asperity will be highly valued. The research on the uncertainty characteristics of the related parameters of asperity are helpful to more accurately predict the strong ground motion characteristics of the future destructive earthquakes. In the process of numerical simulation, the uncertainty of parameters such as the number and position of asperity is mainly considered, and other source parameters are obtained by statistical methods. Empirical Green function method is used as the numerical simulation tool. Xichang earthquake happened 170 years ago, there is no observed data, so there is no way to give the exact intensity characteristics of Xichang earthquake. In this paper, the acceleration data recorded by 32 strong earthquake stations are used as Green function to synthesize the Magnitude 7.5 earthquake, and many numerical simulation possibilities are obtained by setting many kinds of asperity source models combined with the intensity characteristics of modern similar magnitude earthquakes. As a result, the spatial distribution characteristics of ground motion intensity with high probability and the source model of Xichang earthquake prediction based on the uncertainty of asperity parameters are finally obtained. The results show that the results of the source model and numerical simulation can reflect the intensity characteristics of the Xichang M7.5 earthquake; the PGA intensity of the single asperity source model is the largest, and the maximum PGA, 1250gal, appears at station 051XCH. With the increase of the number of asperities, the intensity of ground motion decreases and earthquake duration increases, indicating that the increase of the number of asperities will disperse seismic energy.

Keywords: Xichang earthquake;asperity;ground motion prediction;Green function;numerical simulation

1. Introduction

An earthquake of Magnitude 5.1 occurred in Xichang County, Liangshan Yi Autonomous Prefecture, Sichuan Province (27.70 N, 102.08 E) on Oct. 31st, 2018. Its depth is 19km. The epicenter of this earthquake is located near the eastern boundary fault of Sichuan-Yunnan rhombus block(Fig.1). The main seismotectonic in this area are An-ning river fault, Zemu river fault and Xiaojiang Fault, which are part of the eastern boundary of Sichuan-Yunnan block. In the history of these block boundary faults, strong earthquakes of M ⩾ 7 occurred many times and accompanied by surface rupture of about 100km. For example, the An-ning river fault had an earthquake of M⩾7.5 in Xinhua and Xichang, in 1536. The surface rupture zone starts from Xichang in the South and ends in Mianning in the north, with a length of about 80

km and a maximum co-seismic dislocation of 4m. The Zemu river fault had an earthquake of M ⩾ 7.5 in Xichang and Pugejian in 1850. The surface rupture zone is about 85km, with a maximum co-seismic dislocation of 8m; Xiaojiang fault occurred in the Songming earthquake of M 8.0 in 1833, and formed an earthquake surface rupture zone with a length of more than 120km. Geological and seismic evidences show that the boundary faults of these blocks have the ability to generate earthquakes of M8.0.

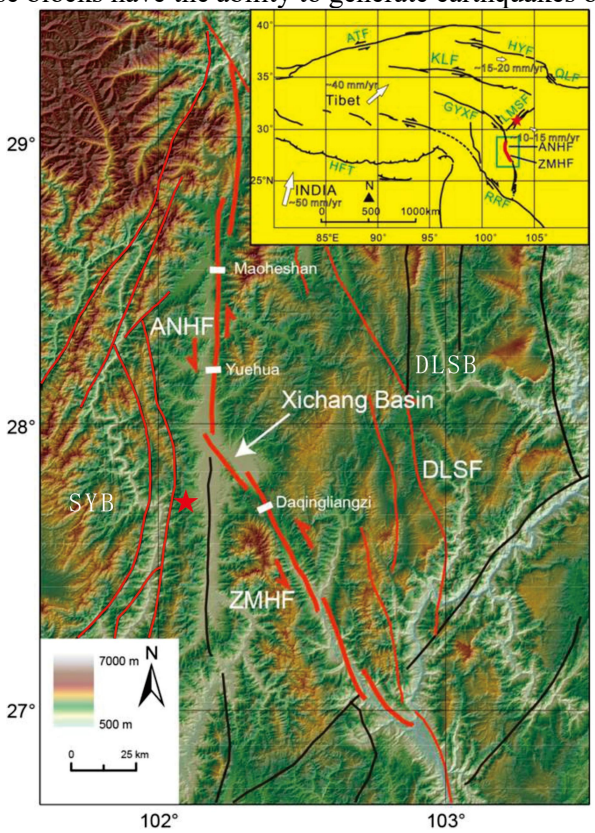

Fig.1 -Seismogenic structure map of Xichang regions. Red line means Fault; red five-star means epicenter; ANHF-Anning River fault, DLSF-Daliangshan fault, DLP-Delipu fault, SYB-Sichuan Yunnan Block, DLSB-Daliangshan Block.(This figure refer from report on direct loss assessment of Xichang earthquake with Ms5.1 in Sichuan Province)

The acceleration time history records of 32 strong motion stations are recorded in the Center of China National Strong Motion Observation Network. The maximum peak acceleration (PGA) appears in the E-W component of 051XCX station, which is 199.1gal (Fig.2). The PGA of E-W component is larger than that of N-S component in the whole earthquake. In this paper, Xichang M7.5 earthquake occurred in 1850 is selected as the target earthquake for numerical simulation. The interval between the two events is more than 170 years, but the focal location of the two events are basically in the same area. We try to regard the Ms5.1 earthquake as the Green function, and use the empirical Green function method to synthesize the large earthquake. The core idea of this method is to use the foreshock or aftershock record of the main earthquake as the Green's function to synthesize the large earthquake (Hartzell, 1978, Irikura, 1983, 1986; Hiroe Miyake, 2003), regarding the source of the large earthquake as a series of sub-earthquake sources, selecting an appropriate aftershock or foreshock record as the Green's function. The small earthquake was equated with the sub-earthquake, and according to a certain rupture mode, take these as the Green's function. The time history of large earthquake is obtained by the superposition of these Green functions(Irikura, 1983,1986; Hiroe Miyake, 2003).

Although this Ms5.1 earthquake is not the aftershock of Xichang earthquake, the location of the two earthquakes is very close. The propagation path and site conditions are very similar to the large earthquake, which can reproduce the strong ground motion characteristics of Xichang earthquake to a certain extent. The

small earthquake records used in empirical Green's function method are generally aftershocks of large earthquakes. Limited by this condition, this method is rarely used in areas lacking seismic records. But with more and more abundant earthquake records, more and more scholars began to use the aftershocks of other earthquakes to synthesize the ground motions of large earthquakes. Kurahashi et al. (2010) successfully simulated the main earthquake record of Wenchuan earthquake with the aftershock record of Japan for the objective reason of not obtaining the aftershock record of Wenchuan earthquake. Li Zongchao et al. (2019) synthesized the Jiuzhaigou M7.0 earthquake with the aftershocks of Wenchuan earthquake and Dingxi earthquake, and evaluated the strength range of stations without earthquake records. HOUSHMANDVIKI (2019) uses the small events that occurred in 2005 (Mw = 4.5), 2012 (Mw = 4.4), 2010 (Mw = 4), and 2007 (Mw = 4) to simulate the 2004 Parkfield earthquake (Mw = 6.1). The strong motion generation areas (SMGA) are estimated to reproduce near-source ground motions in a broadband frequency range of 0.25–10Hz. This study will also accumulate experience for numerical simulation of ground motion in areas and cities with large historical earthquakes and modern small earthquake records, and try to broaden the application scope of empirical Green function method.

The prediction of earthquake intensity is of great significance to the seismic fortification of buildings in the area without destructive earthquake and the future urban planning. It is a very important basic work in earthquake prevention and mitigation. It is also a very practical and meaningful research direction to use the aftershock records of other major earthquakes as Green's function to predict the future ground motion of a destructive major earthquake in a certain place. With the continuous improvement of the method and more and more experience of simulation, it is sure to provide a practical and reliable reference for seismic fortification of buildings.

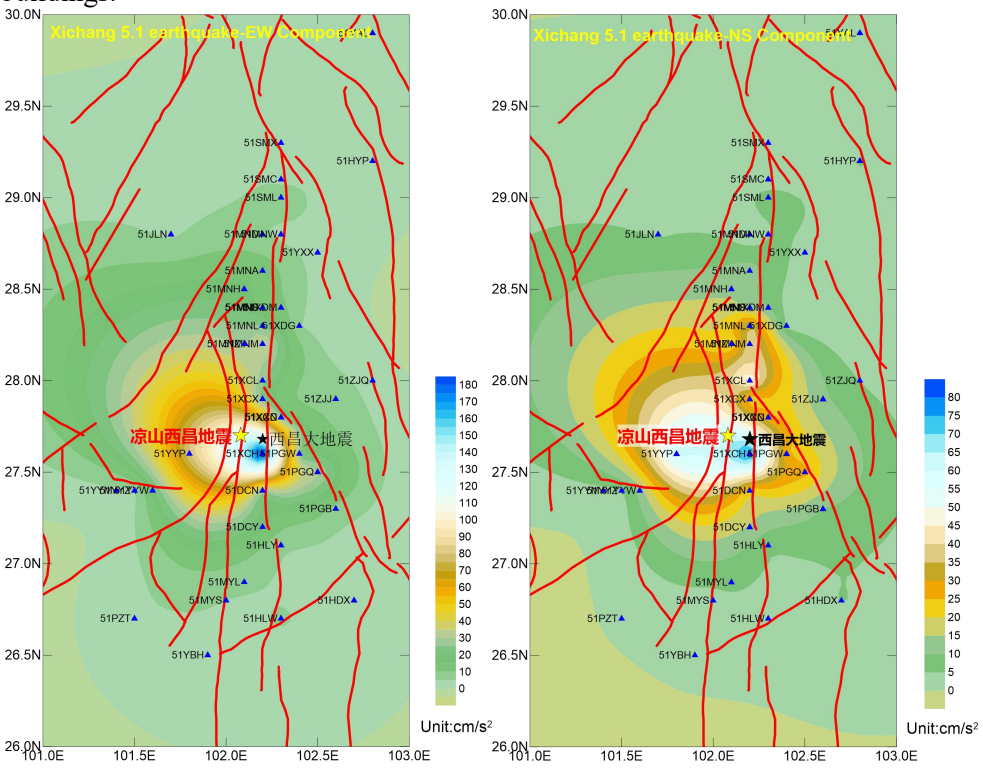

(a) (b)

Fig.2- The PGA distribution map of Xichang Ms5.1 earthquake. (a) means the E-W component of PGA distribution while (b) is N-S components. Red lines are faults;Yellow five-pointed star was the epicenter of Xichang Ms5.1 earthquake while the black five-pointed star was the epicenter of Xichang Ms7.5 earthquake. The blue triangle was stations.

2. Numerical simulation method and earthquake source parameters

2.1 Numerical Simulation Method

The empirical Green function method, which uses small earthquakes as Green functions, was first proposed by Hartzell (1978). Small earthquake records include the influence of the complexity of the source's rupture process, propagation medium and site conditions. Therefore, the complexity of the source, propagation medium and site conditions is also considered in the large earthquake records synthesized by small earthquake records, and the calculation difficulty of the theoretical Green's function can also be overcome (Hartzell, 1978). Many seismologists, including Kanamori (1979), Dan *et al*. (1989), and Irikura (1983, 1986), have since revised this method. In this article, we use the version revised by Irikura to synthetic the large earthquake. We assume that a major earthquake hypocenter consists of many minor earthquake hypocenters. Accordingly, an appropriately small earthquake is chosen as the ground motion response caused by a point source, and the small earthquake is considered an empirical Green function. An empirical Green function is based on a scaling law of fault parameters for large and small events (Kanamori and Anderson, 1975). The expressions for a synthetic main shock and aftershock (Irikura 1986; Hiore Miyake *et al*. 2003) are shown in Eqs. 1, 2 and 3, respectively (Hiroe Miyake *et al*. 2003):

$$U_0(x,t)=\sum_{i=1}^{N}\sum_{j=1}^{N}\frac{r_s}{r_{ij}}F(t)*(C\cdot u_s(t)) \quad (1)$$

$$F(t)=\delta(t-t_{ij})+\frac{1}{n'}\sum_{k=1}^{(N-1)n'}[\delta\{t-t_{ij}-\frac{(k-1)T}{(N-1)n'}\}] \quad (2)$$

$$t_{ij}=\frac{r_{ij}-r_0}{V_s}+\frac{\xi_{ij}}{V_r} \quad (3)$$

where $U_0(x,t)$ is the synthetic record of a major earthquake, $u_s(t)$ is the Green function; r_{ij} and r_s are the hypocentral distances of the element earthquake and aftershock, respectively; r_0 denotes the distance from the site to the starting point of rupture on the fault plane of the large event; ξ_{ij} represents the coordinates (i, j) of the element source; T is the rise time for the large event, which is defined as the duration of the correction function; $F(t)$ is the correction function used to adjust the large and small events (Hiroe Miyake et al. 2003); n' is an appropriate integer for suppressing the artificial periodicity of n and adjusting the interval of the sampling rate (Hiroe Miyake *et al*., 2003); V_s and V_r are the S-wave velocity close to the source area and the rupture velocity along the fault plane, respectively; and N and C are ratios of the fault dimensions and stress drops, respectively.

2.2 Earthquake source parameters

The earthquake data used in this paper are all from the National Strong Motion Observation Network Center. The acceleration time history records of 32 strong motion stations (Fig.1) are selected. We refer to Somerville's (1999) research results for the total area parameters of the asperity, that is, the area of the asperity accounts for 22% of the total fault rupture area, and the seismic moment of the asperity accounts for 44% of the total seismic moment. In this paper, the area parameter of the asperity is 2156 km2, and the seismic moment of the asperity is 2.28e+26 dyne.cm. We assume that the stress drop on the asperity is homogeneous. Other parameters of large and small earthquakes are shown in Table 1. Because the focal mechanism parameters of the main earthquake cannot be verified, the focal mechanism parameters of the small earthquake are referred to. S-wave velocity refers to the velocity structure of Sichuan Yunnan test site(Yao, H. J，2019). The rupture velocity of fault plane is 0.72 times of S-wave velocity.

Table 1 -Source parameters of earthquakes

Earthquake magnitude	epicenter	Depth	Seismic moment (dyne.cm)	S-wave velocity T-(km/s)	rupture velocity (km/s)	strike	dip	rake
7.5	(102.2E, 27.68N)	15km	5.19E+26	3.6	2.59	340	80	3
5.1	(102.08E, 27.70N)	19km	1.51E+24	3.6	2.59	340	80	3

2.3 Asperity location uncertainty

For the occurred earthquakes (Such as, Wenchuan earthquake, Lushan earthquake, Jiuzhaigou earthquake, etc.), the focal rupture process and the spatial location distribution of the asperity can be confirmed by the deterministic method. The spatial location of the asperity is determined. Considering the difference of the propagation time and path of the S-wave, the velocity of the rupture on the asperity, etc., the superposition time of each asperity can be calculated duration delay (Kurahashi and Irikura, 2010; Koketsu, 2009; Chen Xia 2015). The location of the asperity on the fault plane is random and uncertain for the earthquake that has not occurred. Different asperities can be continuous or discontinuous. Therefore, it is difficult to give an exact value when the asperity is superimposed, and the duration delay obtained by the different station is also unknown. For the source model with multiple asperity, we give the approximate time delay between different asperity(Fig.5, shown by two asperities), mainly considering the time delay of S-wave and the time delay of rupture process on the asperity fault plane. The time delay of each station point is shown in equation 4.

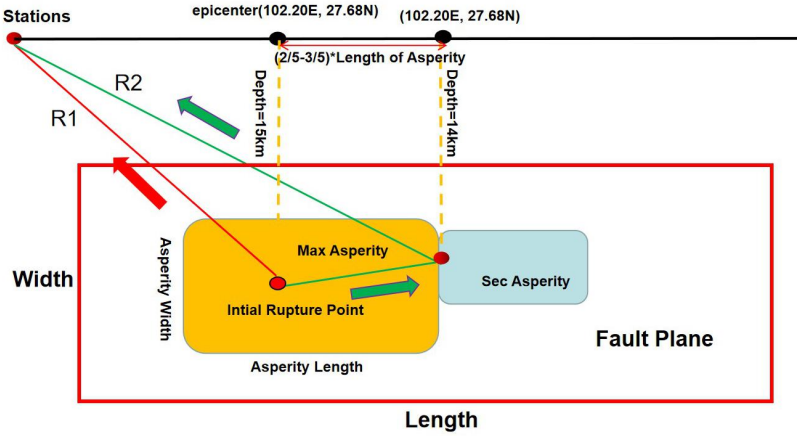

Fig.5- Duration delay calculating model

$$\Delta t = D_{rupture}/Vr + R_{asperity}/V_s - r_0/V_s \qquad (4)$$

Where, $D_{rupture}$ is the distance from the initial rupture point of the maximum asperity to the secondary asperity. $R_{asperity}$ is the distance from the initial rupture point of the secondary asperity to a station, and R_0 is the distance from the initial initial rupture point of the maximum asperity to a station. In addition, we will give the value range of time interval for different numbers of asperities, rather than a fixed time interval. Because the spatial distribution range of asperities for unknown or historical earthquakes cannot be known, it is more appropriate to give a reasonable value range of time delay.

3. Numerical simulation result

3.1 The PGA distribution characteristic of different asperity-source model

We simulated the acceleration time history and PGA of 32 stations while the asperity number is 1 or 2, respectively.Then 32 stations are interpolated and fitted to obtain the spatial distribution characteristics of the ground motion of each asperity source model shown in Fig.6 and Fig.7. It should be noted that in the two asperity models, we assume that there are two initial rupture points of the largest asperity, i.e. the position close to the South and the north of the largest asperity, and the numerical simulations are carried out respectively. For the single asperity model, the maximum PGA of E-W component is 1150 gal, and the maximum PGA of N-S component is 1250 Gal. For the two asperities model, the maximum PGA is 1005 gal when the initial position is on the south side, and the maximum PGA is 1024 gal when the initial initial position is on the north side.

(a)

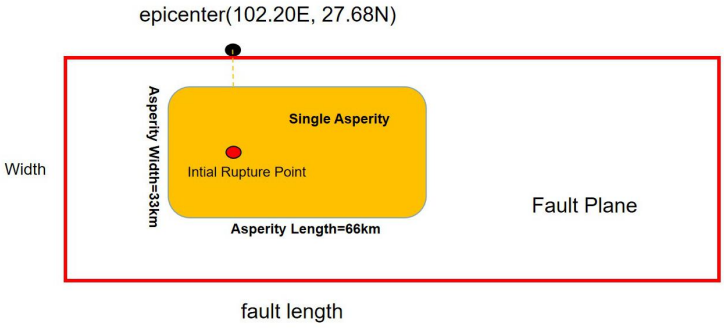

(b)

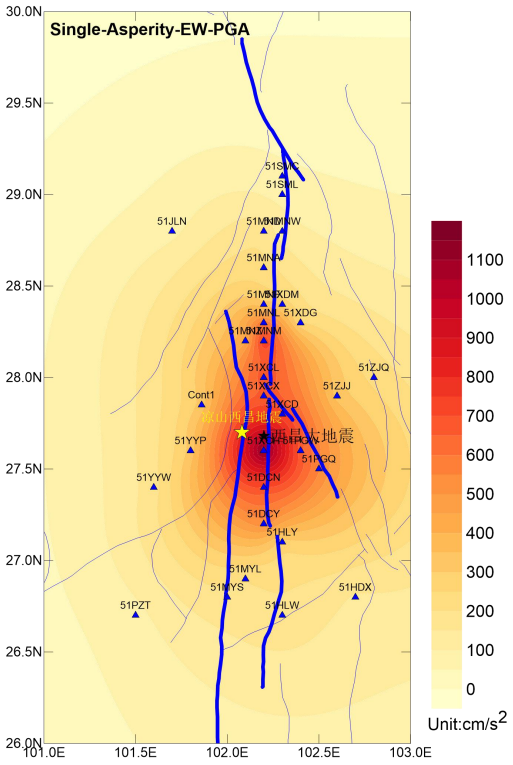

(c)

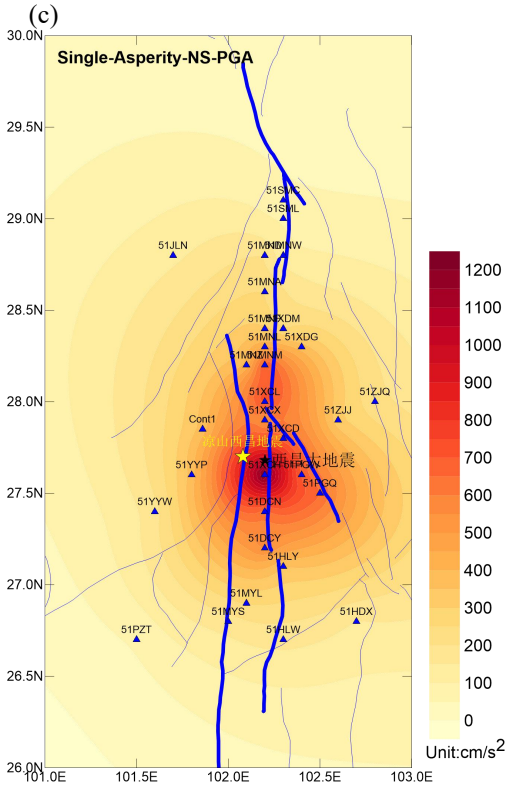

Fig.6- The source model and PGA distribution of single asperity model. (a) is the single asperity source model; (b) is the PGA distribution map of E-W component. The max PGA of E-W component is 1150gal; (c) is the PGA distribution map of N-S component. The max PGA of N-S component is 1250gal.

(a)

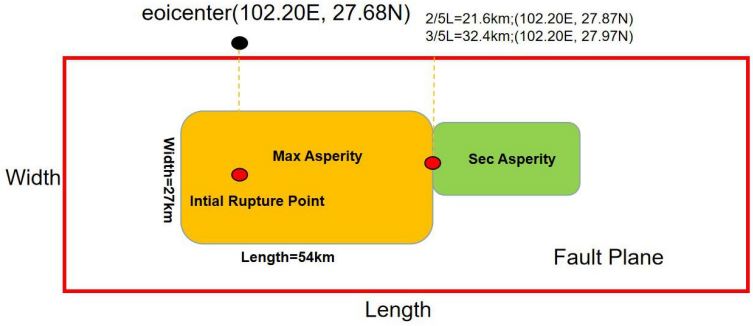

(b) (c)

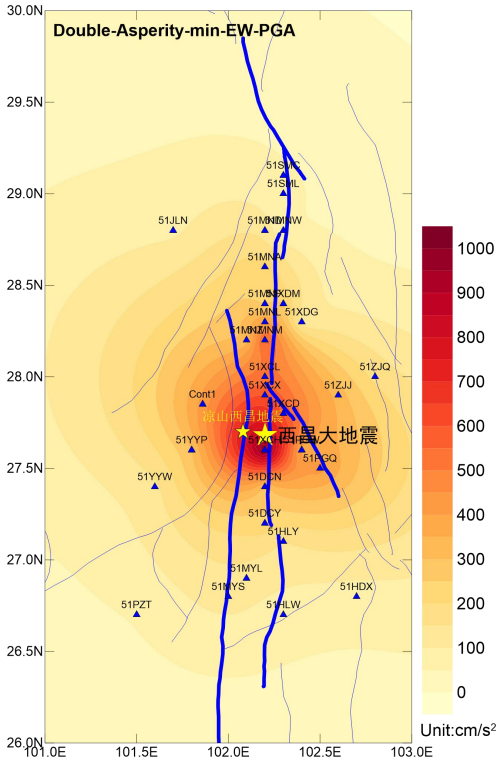

(d)

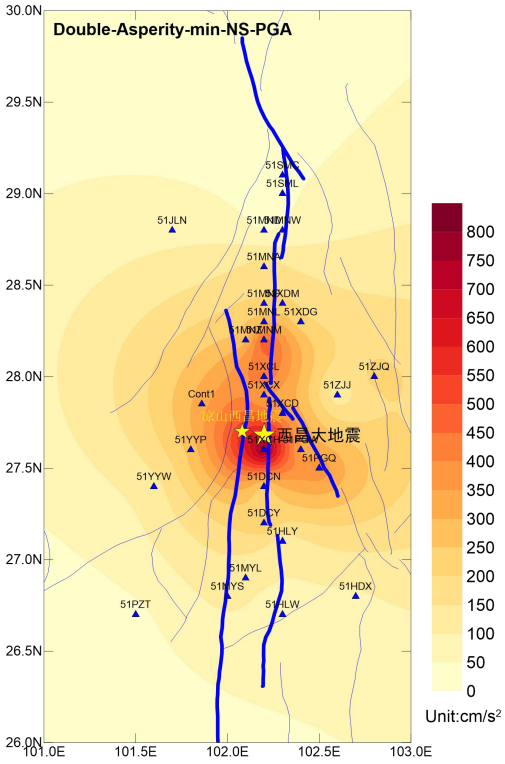

(e)

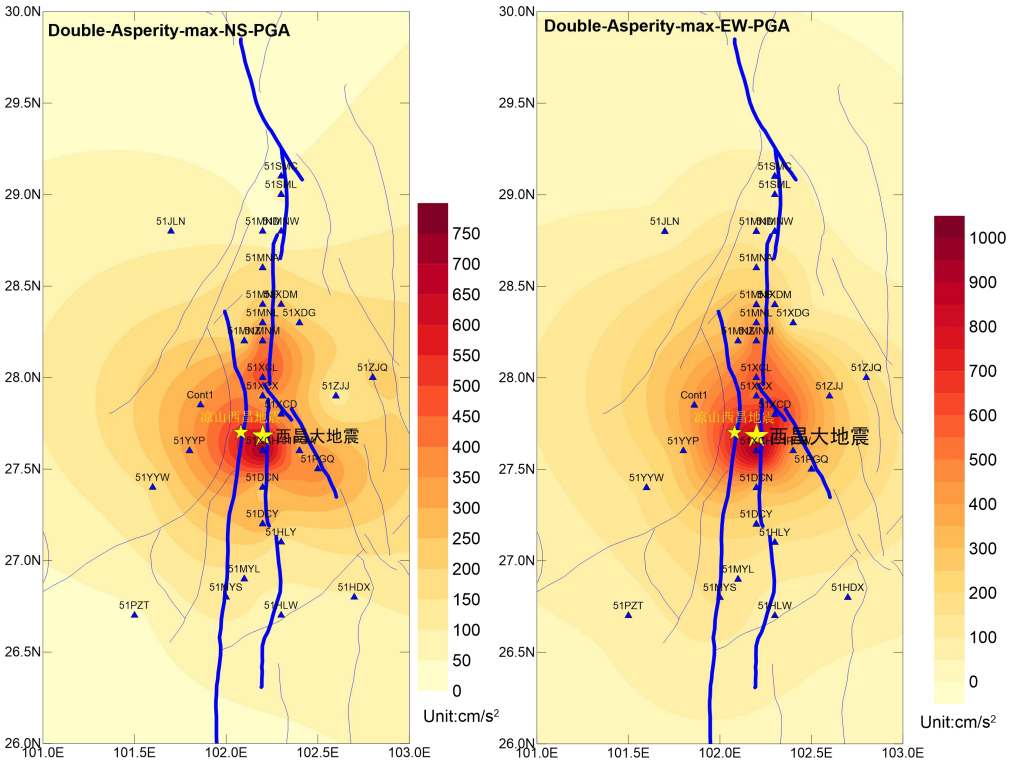

Fig.7- The source model and PGA distribution of two asperity model with different initial rupture point. (a) is the two asperity source model; (b) is the PGA distribution map of E-W component while the initial rupture was in south part of the largest asperity. The max PGA of E-W component is 1005 gal; (c) is the PGA distribution map of N-S component while the initial rupture was in south part of the largest asperity. The max PGA of N-S component is 778 gal; (d) is the PGA distribution map of E-W component while the initial rupture was in north part of the largest asperity. The max PGA of E-W component is 1024 gal; (e) is the PGA distribution map of N-S component while the initial rupture was in north part of the largest asperity. The max PGA of N-S component is 815 gal.

3.2 Synthetic acceleration and response spectrum

Limited by the length of this paper, only one station (station DCN)'s acceleration time history and response spectrum of different asperity source models are listed here. The PGA of single asperity model is larger than that of double asperities model, but the duration time is shorter than that of double asperity model(Fig.8). The response spectrum amplitude of single asperity is also higher than that of double asperity model(Fig.9).

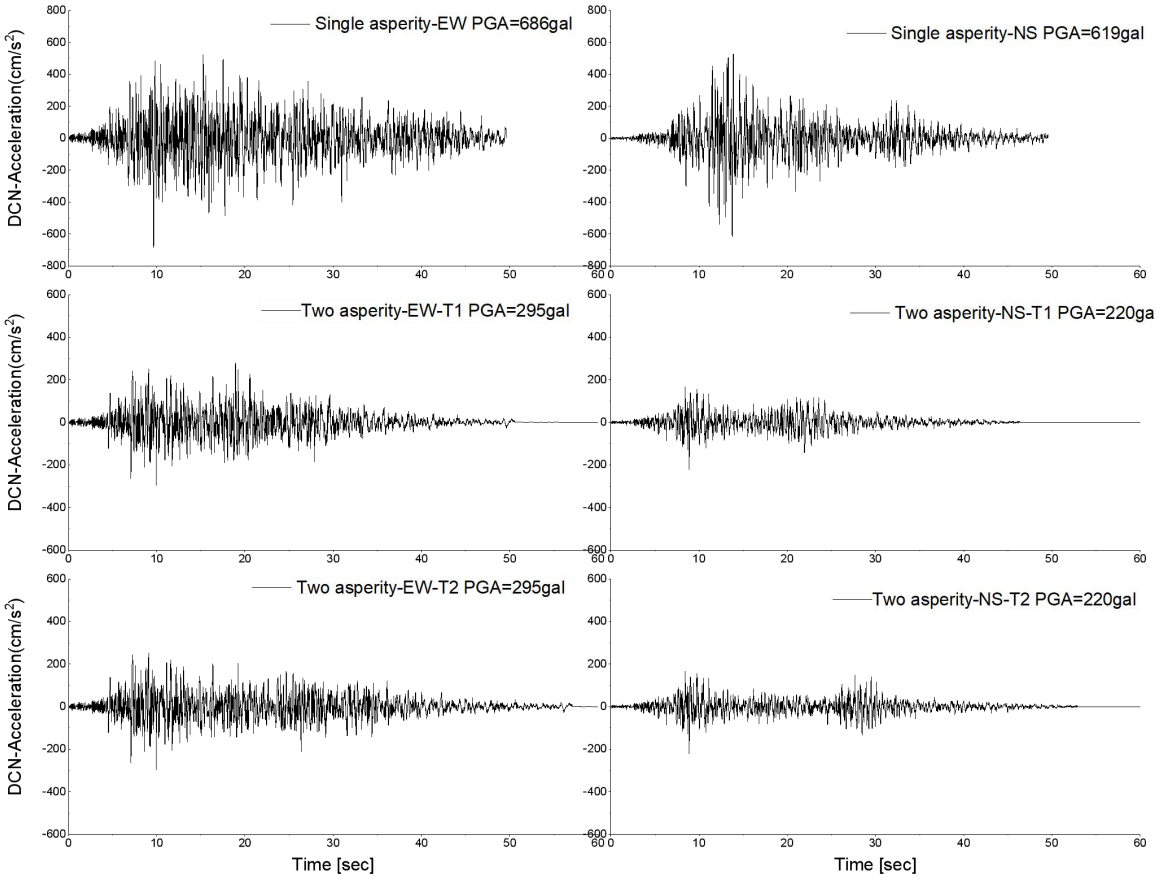

Fig.8- the acceleration of station DCN with different asperity source model. The epicenter of station DCN is 31.14 km. The PGA of E-W component with single asperity is 689gal; The PGA of N-S component with single asperity is 619 gal. The PGA of E-W component with two asperity is 295 gal. The PGA of N-S component with two asperity is 220 gal. The T1 means initial rupture point locating at the south of largest asperity while T2 means initial rupture point locating at the north of largest asperity.

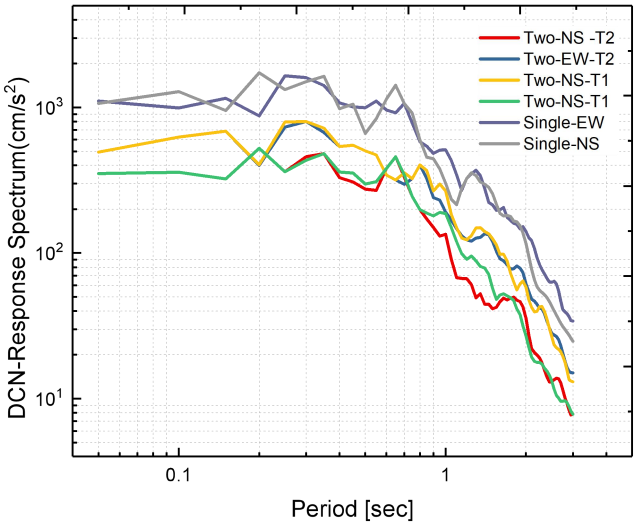

Fig.9 -The response spectrum of station DCN with different asperity model. The damp is 5.0%.The epicenter of station is 31.14km. The T1 means initial rupture point locating at the south of largest asperity while T2 means initial rupture point locating at the north of largest asperity. The amplitude of single asperity response spectrum is higher than two asperity.

4. Conclusion and Prospect

By analyzing and comparing the seismic intensity characteristics of all asperity source models, combined with the seismic characteristics of destructive large earthquakes with similar magnitudes in recent ten years, we can get the following conclusions:

（1）The location of the asperity and the Xichang basin area have relatively large intensity of ground motion；

（2）With the increase of the number of asperity, the intensity of ground motion decreases near the epicenter and Xichang Basin;

（3）The spatial distribution characteristics of the ground motion intensity of each asperity model is generally north-south oriented, elliptical diffusion attenuation. The ground motion intensity of Qionghai area and its surrounding areas is also relatively large, reflecting the amplification effect of the basin topography on the ground motion；

（4）We think that it is more likely that Xichang earthquake has single or two asperity. The results of the asperity source model and numerical simulation can reflect the intensity characteristics of the Xichang M7.5 earthquake. With the increase of the number of asperity, the intensity of the ground motion decreases. The increase of the number of asperity will disperse the seismic energy. The real ground motion intensity should be between the two kinds of asperity model.

The accuracy of the simulation results: we give the value range of each asperity model. Considering the uncertainty of the location of the asperity, the real seismic intensity range should be between the two assumed initial rupture point. The Ms5.1 earthquake occurred in the same place as the historical earthquake, and the small earthquake records are basically consistent with the historical earthquake in terms of the influence of the propagation path and site conditions. The empirical Green's function method has been used for many times to simulate the occurred earthquakes, and the results are widely recognized. It is relatively mature method and the simulation results are reliable. Compared with the modern earthquake records with the same magnitude and the characteristics of ground motion intensity, such as Wenchuan earthquake, Lushan earthquake, Tangshan earthquake, Jiji earthquake, etc., the simulation results have the strength characteristics and main energy duration characteristics of destructive large earthquakes. The simulation results show the possible value range, considering the uncertainty of source parameters, and give the more likely intensity characteristics of historical earthquakes. To sum up, the source model with Ms5.1 earthquake as Green's function and considering the uncertainty of asperity parameters is used to simulate the intensity characteristics of Xichang earthquake. The results have good reference value.

4. Acknowledgements

This work was supported by the National key research and development program(2017YFC1500205) and the special fund of the Institute of Geophysics, China Earthquake Administration (DQJB17T04, DQJB19A0131, DQJB19A0133). Data for this study are provided by Engineering Mechanics, China Earthquake Administration. The focal mechanics of Ms5.1 earthquake was from the https://www.globalcmt.org/CMTsearch.html.)

5. Copyrights

6. References

[1] Hartzell S H. 1978. Earthquake aftershocks as Green's functions[J]. Geophysical Research Letters, 5(1): 1-4.

[2] Haskell N A. 1969. Elastic displacements in the near-field of a propagating fault[J]. Bulletin of the Seismological Society of America, 59(2): 865-908.

[3] Hanks T C, Kanamori H. 1979. A moment magnitude scale[J]. Journal of Geophysical Research B, 84(B5): 2348-2350.

[4] Irikura K. 1986. Prediction of strong acceleration motion using empirical Green's function[C]//Proc. 7th Japan Earthquake Engineering Symposium. : 151-156.

[5] Miyake, H., Iwata, T., & Irikura, K. 2003. Source characterization for broadband ground-motion simulation: Kinematic heterogeneous source model and strong motion generation area. Bulletin of the Seismological Society of America, 93(6), 2531-2545.

[6] Kamae K, Irikura K, Pitarka A. A technique for simulating strong ground motion using hybrid Green's function[J]. Bulletin of the Seismological Society of America, 1998, 88(2): 357-367.

[7] Irikura K. 1983. Semi-empirical estimation of strong ground motion during large earthquake[J]. Bull Disas Prev Res，33：151–156.

[8] Irikura K, Miyake H. Recipe for predicting strong ground motion from crustal earthquake scenarios[J].Pure and Applied Geophysics, 2011, 168(1-2): 85-104.

[9] Irikura K, Kamae K. Estimation of strong ground motion in broad-frequency band based on a seismic source scaling model and an empirical Green's function technique[J]. Annals of Geophysics, 1994,37(6).

[10] Kurahashi S, Irikura K. Characterized source model for simulating strong ground motions during the 2008 Wenchuan earthquake[J]. Bulletin of the Seismological Society of America, 2010, 100(5B):2450-2475.

[11] Irikura K, Miyakoshi K, Kamae K, Yoshida K, Somei K, Kurahashi S, Miyake H. 2017. Applicability of source scaling relations for crustal earthquakes to estimation of the ground motions of the 2016 Kumamoto earthquake[J]. Earth Planets Space，69： 10.

[12] Kanamori H. A semi-empirical approach to prediction of long-period ground motions from great earthquake [J]. BSSA,1979,69(6):1654-1670.

[13] Yao, H. J., Yang, Y., Wu, H. X., Zhang, P. and Wang, M. M. (2019). Crustal shear velocity model in Southwest China from joint seismological inversion. CSES Scientific Products., doi:10.12093/02md.02.2018.01.v1

[14] ZongChao L, MengTan G, XueLiang C, et al. Simulation of ground motion by the 2017 Jiuzhaigou Ms 7. 0 earthquake and estimation of ground motion intensity in the Zhangzha Town[J]. CHINESE JOURNAL OF GEOPHYSICS-CHINESE EDITION, 2019, 62(7): 2567-2581.

[15] Koketsu K, Yokota Y, Ghasemi H, et al. Source process and ground motions of the 2008 Wenchuan earthquake[C]//Proceedings of International Conference on Earthquake Engineering—The First Anniversary of Wenchuan Earthquake. 2009: 11-12.

[16] Xia C, Zhao B, Horike M, et al. Strong Ground Motion Simulations of the M w 7.9 Wenchuan Earthquake Using the Empirical Green's Function Method[J]. Bulletin of the Seismological Society of America, 2015, 105(3): 1383-1397.

[17] HoushmandViki, A., H. Hamzehloo, H. Miyake, and A. Ansari (2019). Estimation of strong motion generation area for the 2004 Parkfield earthquake using empirical Green's function method, Pure Appl. Geophys., https://doi.org/10.1007/s00024-019-02327-9.

[18] Somerville P, Irikura K, Graves R, et al. Characterizing crustal earthquake slip models for the prediction of strong ground motion[J]. Seismological Research Letters, 1999, 70(1): 59-80.

[19] Dan K, Watanabe T, Tanaka T. A semi-empirical method to synthesize earthquake ground motions based on approximate far-field shear-wave displacement[J]. Journal of structural and construction Engineering (Transactions of AIJ), 1989, 396: 27-36.

